Robust Model-Based Fault Detection for a Roll Stability Control System

Li Xu and H. Eric Tseng

***Abstract*—Fault management is critical for a vehicle active safety system. Since a sensor fault may not always be detectable by a sensor self-test or an electronic monitoring system whose detection often relies on out-of-range signals, a redundancy check is warranted for the detection of an in-range signal fault. In this paper, an in-vehicle roll rate sensor failure detection scheme utilizing analytical redundancy is presented. The vehicle is assumed to be equipped with a steering wheel angle sensor, a yaw rate sensor, a lateral accelerometer, and wheel speed sensors in addition to the roll rate sensor. Due to the wide variation of vehicle dynamics under a vast operating range, such as various and dynamically changing road super-elevations and road grades, the detection of a roll rate signal fault using analytical redundancy is particularly challenging. These challenges, as well as the robustness and performance of the proposed scheme are discussed. The robust performance of the proposed scheme, over model uncertainties and road disturbances, is illustrated analytically and validated through experimental test data. The analytical illustrations include three elements: a robust estimation of the vehicle roll angle, a dynamic compensation of both electrical and kinematics-induced biases in the roll rate signal, and a directionally sensitive design of a robust observer which decouples the model uncertainties and disturbances from the fault. The experimental verifications of no false positive and/or no false negative were taken with a variety of maneuvers and road conditions on several vehicle test platforms.**

***Index Terms*—Electronic stability control, fault diagnosis, road vehicle control, sensor error compensation, state estimation.**

I. Introduction

RECENTLY, Ford Motor Company has developed a brake actuation systems to enhance on-road vehicle roll stability [1]. The Ford Roll Stability Control (RSC) System utilizes a sensor set to monitor the dynamic condition of a vehicle and a controller to distribute brake pressure for reducing lateral tire forces that contribute to the detected roll instability. The sensor set includes four wheel speed sensors, a steering wheel angle sensor, a longitudinal acceleration sensor, a lateral acceleration sensor, a yaw rate sensor, and a roll rate sensor [1]. The roll rate sensor is the only additional sensor on top of the Electronic Stability Control (ESC) System which enhances the yaw stability of the vehicle [2], and can be used to provide RSC with critical feedback information. Failures of the roll rate sensor in an RSC equipped vehicle, therefore, must be rapidly diagnosed to ensure proper system activations.

Manuscript received May 30, 2006; revised October 30, 2006. Manuscript received in final form December 7, 2006. Recommended by Associate Editor I. Haskara.

The authors are with the Research and Advanced Engineering, Ford Motor Company, Dearborn, MI 48124 USA (e-mail: lxu9@ford.com; htseng@ford.com).

Digital Object Identifier 10.1109/TCST.2006.890287

In this paper, a fault detection scheme using analytical redundancy that offers cost efficiency (versus the one using hardware redundancy) is considered. Fault detections using analytical redundancy can be categorized into knowledge-based approaches and model-based approaches. Both approaches generally utilize any or all of the following *a priori* knowledge [3]: 1) a model of the normal process, e.g., a nominal plant that does not include disturbances/faults; 2) a model of the observed process, e.g., a model (which may include disturbances/faults) identified by the observed process using state or parameter estimation techniques; and 3) models of the faulty process, e.g., fault signatures. As suggested in [3], it is considered that a knowledge-based detection approach relies mostly on the faulty process, while a model-based detection approach emphasizes the design of the observed process. Among the model-based detection processes, a robust observer design using eigenstructure assignment is believed to offer a better robustness over voting schemes, Kalman filter-based approaches, etc. The impact of an inaccurate model on Kalman filter-based approaches was examined by [4] and the robustness advantage of robust observer design was suggested in [5]. For roll rate sensor fault detection, this is particularly appealing due to large unknown roll disturbances and model uncertainties encountered in a passenger vehicle.

While fault detection methodologies using eigenstructure assignment have previously been developed for other systems [5], [6], the roll rate fault detection problem at hand poses a few unique challenges. The vehicle roll angle, which is used to cross check the roll rate signal, is not directly measured. Therefore, in addition to finding a proper vehicle roll model and constructing a robust observer using this methodology, the vehicle roll angle has to be estimated. Since estimation errors are inevitable, the roll rate sensor fault must be separated from such estimation errors in the residual calculation. Lateral accelerometer-based roll angle estimations have been investigated in the literature [7] and [8]. In [7], it was concluded that the estimates cannot be accurate when there is a mismatch in parameters (which can be induced by payload) or when road bank angle disturbances are present. Reference [8] also described the accelerometer-based estimate as unreliable when road noise overwhelms. Another challenge arises from the kinematics bias of the roll rate sensor. It contains a significant bias when the vehicle is turning (or yawing) on an inclined road, picking up the product of yaw rate and pitch angle. Since this is induced by the kinematics relation between the inertial frame and the rotating (vehicle body) frame, the sensing bias is legitimate. That is, the bias cannot be considered as a sensor fault despite the fact that it needs to be compensated for the use of the RSC System. Furthermore, due to the wide variation of vehicle dynamics under a vast operating range, such as various and dynamically changing road super-elevations

and road grades, the magnitude of disturbances existing in the roll rate signal and roll angle estimate is significant and the detection of a roll rate signal fault using analytical redundancy is particularly challenging.

There are three main contributions in this paper. First, it provides an innovative way of fault detection (as opposed to the usual voting scheme [2]) for an actual in-production automotive application. Second, it links the fault detection theory with the actual application through a proper design and model selection. The design eliminates the need of parameter calibration or adaptation due to the decoupling of model uncertainties from sensor fault. Third, it addresses the remaining challenges discussed in the previous paragraph. That is, it provides additional fault separation capability by eliminating the legitimate kinematics bias, enhancing roll angle estimate, and further separating the sensor fault from estimation error in the frequency domain.

The paper is organized as follows. In Section II, the theory behind the selected fault detection strategy is briefly reviewed. Section III shows detailed steps of bridging the gap between the theory and a successful implementation, which includes selection of appropriate vehicle model, compensation of legitimate electrical and kinematics sensor biases, and construction of the redundant roll angle signal. Section IV utilizes simulations to illustrate the robustness of the designed observer despite simulated model uncertainties, unmodeled dynamics, and errors from the redundant roll angle signal. Section V further demonstrates the overall robust performance of the implementation with experimental results.

II. Robust Fault Observer Using Eigenstructure Assignment

Model-based fault diagnosis approach has received considerable attention during the last two decades [3], [9]–[11]. The most common model-based fault detection scheme involves the use of an observer. These include Kalman filter approaches that utilized assumed models and anticipated fault behaviors [4], [12]; stochastic approaches with Whiteness and Chi-squared tests of the residuals of Kalman filter [13]; a generalized likelihood ratio test which relies on a correlation of the observed residual with presumed fault signatures [9]; and fault-sensitive filters that amplify certain direction in the state space in which the fault resides [5], [6], [11]. Considering the significant variations a vehicle may experience in practice, there is a need to develop robust fault detection algorithms in which the sensor fault is decoupled from model uncertainties and disturbances, and the residual is sensitive only to sensor fault. One way to achieve this is to use the eigenstructure assignment approach [5], [6], [14].

Consider a class of linear systems, in which the system uncertainties can be summarized as an additive unknown disturbance term in the dynamic equation described as follows:

$$\begin{aligned} \dot{x} &= Ax + Bu + E\tilde{d} \\ y &= Cx + Du + f_s \end{aligned} \tag{1}$$

where x is the state vector, u is the input vector, y is the output vector, and f_s is the sensor fault. $\tilde{d}$ denotes disturbances acting upon the system, and its distribution matrix E is assumed to be known. A, B, C, and D are known system matrices with proper dimensions. Let the state and output estimations be $\hat{x}$ and $\hat{y}$. A state observer for system (1) is given by

$$\begin{aligned} \dot{\hat{x}} &= A\hat{x} + Bu + K(y - \hat{y}) \\ \hat{y} &= C\hat{x} + Du \end{aligned} \tag{2}$$

where K is the observer gain. Define the state estimation error as $e = x - \hat{x}$. The error dynamics become

$$\dot{e} = \dot{x} - \dot{\hat{x}} = Ax + Bu + E\tilde{d} - A\hat{x} - Bu - K(y - \hat{y}) = (A - KC)e + Ef_s. \tag{3}$$

Now the residual generator can be formed by premultiplying the output estimation error with a weighting matrix W as

$$r = W(y - \hat{y}) = W(Cx + Du + f_s - C\hat{x} - Du) = We. \tag{4}$$

The Laplace transformed residual response to faults and disturbances is thus given by

$$r(s) = WC(sI - A_c)^{-1}E\tilde{d}(s) + [WC(sI - A_c)^{-1}E + W]f_s(s) \tag{5}$$

where s is the Laplace operand and $A_c = A - KC$ is the closed-loop matrix. The disturbance decoupling condition can be easily seen from before as

$$G_{rd}(s) = WC(sI - A_c)^{-1}E = 0. \tag{6}$$

The problem is now reduced to that of finding K and W such that (6) is satisfied and A_c is stable. The assignment of the observer's eigenvectors and eigenvalues is a direct way to solve this problem [6].

Theorem 1: If $WCE = 0$ and all rows of the matrix WC are left eigenvectors of A_c corresponding to p eigenvalues of A_c, then (6) is satisfied [6]. p is the dimension of the residual.

This can be seen from the following:

$$WC(sI - A_c)^{-1}E = WC\left(\sum_{i=1}^{n} \frac{v_i l_i^T}{s - \lambda_i}\right)E \tag{7}$$

where v_i and l_i^T are right and left eigenvectors corresponding to λ_i which are eigenvalues of A_c. n is the order of matrix A_c. Let $WC = [l_1 \cdots l_p]^T$. Since right and left eigenvectors are orthogonal to each other, $WCv_i = 0, \forall i = p+1, \cdots, n$. The decoupling condition (6) can then be written as

$$WC(sI - A_c)^{-1}E = WC\left(\sum_{i=1}^{p} \frac{v_i l_i^T}{s - \lambda_i}\right)E. \tag{8}$$

But it was assumed that $WCE = 0$, i.e., $l_i^T E = 0$, $\forall i = 1, \cdots, p$, which gives $G_{rd}(s) = 0$.

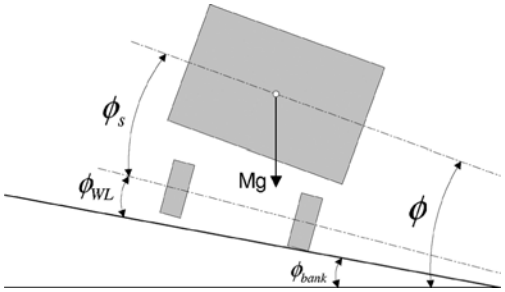

Fig. 1. Vehicle on a banked road.

III. Robust Observer for Roll Rate Fault Detection

A. Plant Model and Robust Observer Design

In order to utilize the observer design technique previously discussed, the selection of a proper observed plant model is a significant design step. While many models describing vehicle roll dynamics are available in the literature [15] and [16], they are not developed for fault detection purposes. On the one hand, these models are all based on multibody dynamics which is highly nonlinear and cannot be utilized to formulate the robust fault observer. On the other hand, they are not sophisticated enough to handle road super-elevations well. Therefore, it is essential to find a model that meets the necessary conditions of Theorem 1. Furthermore, it would be advantageous if the model's parametric uncertainties lie in the same subspace (of the state space) as the external disturbances.

To facilitate the robust observer design, a simple linear time-varying roll model incorporating both kinematics and dynamics relationships is chosen as follows:

$$\frac{d}{} \qquad (9)$$

where ϕ and $\dot{\phi}$ represent the Euler roll angle and roll rate of the vehicle, respectively; the Euler roll angle includes suspension roll angle $\phi_{\boldsymbol{s}}$, wheel lift roll angle $\phi_{\boldsymbol{WL}}$, and road bank angle $\phi_{\mathbf{bank}}$ (Fig. 1). k and c are the nominal values of effective roll stiffness and damping coefficient, which include suspension geometry and other kinematics effects and have been normalized by vehicle roll moment of inertia. Δk and Δc represent parametric uncertainties and/or nonlinearities which may further be time-varying, and d represents any external disturbances (e.g., roll moment from lateral force, road excitation, or from the super-elevation of the road) applied to the vehicle. The output y is selected as follows:

$$y = \begin{bmatrix} \phi \\ \dot{\phi} \end{bmatrix} + \begin{bmatrix} f_\phi \\ f_{\dot{\phi}} \end{bmatrix} \qquad (10)$$

where f_ϕ and $f_{\dot{\phi}}$ denote possible error contained in the roll angle and roll rate signal, respectively. The inclusion of the roll angle signal in the previous output equation is necessary, otherwise, only a trivial solution can be found to satisfy the disturbance decoupling condition (6). This, therefore, necessitates the estimation of the roll angle, since it is not measured in the vehicle.

While the model representation is in a simple format, the model parameters can be nonlinear and time-varying in order to capture the roll dynamics under various driving conditions. For example, constant effective roll stiffness and damping coefficient may be sufficient to describe small suspension roll motions while these parameters may have to be nonlinear in order to reflect vehicle roll during large suspension motions. Moreover, the effective roll stiffness and damping drop significantly when a vehicle stays on a banked road or when a wheel lifts off the ground.

Noting that both parametric uncertainties and disturbances appear in the second equation of (9), the roll model can be rewritten as

$$\begin{aligned} \dot{x} &= Ax + E\tilde{d} \\ y &= C(x + f_s) \end{aligned} \qquad (11)$$

where

$$\qquad (12)$$

$C = I_2$, and $\tilde{d} = d + \Delta k\phi + \Delta c\dot{\phi}$.

The design objective is to detect the roll rate sensor fault $f_{\dot{\phi}}$ which is an offset or drift during vehicle operations in spite of various model uncertainties.

Assumption: The failure detection scheme proposed in this paper, assumes all the reference signals (vehicle velocity, yaw rate, lateral acceleration, steer wheel angle) being used to cross check the roll rate signal are healthy or a fault warning will be received within a precalibrated time should one or more signal faults occur. This assumption is based on the fact that RSC is a system built on top of an ESC system. The source of the reference signals is supposed to be well monitored by ESC, not unlike ESC assumes the wheel speed sensor monitoring as the responsibility of ABS module.

Note that (11) belongs to the class of systems described by (1) (with $B = 0$ and $D = 0$). Thus, the robust observer design presented in Section II can be applied to generate a scalar residual which is insensitive to both parametric uncertainties and disturbances

$$\qquad (13)$$

where W and K are found to be

$$W = [1\ 0], \qquad K = \begin{bmatrix} \lambda_1 & 1 \\ -k & -c + \lambda_2 \end{bmatrix}. \qquad (14)$$

λ_1 and λ_2 are two positive design parameters. It can be verified that the observer poles (or eigenvalues of A_c) are placed arbitrarily at $-\lambda_1$ and $-\lambda_2$, and the necessary conditions of Theorem 1 are satisfied.

B. Roll Angle Estimation

There remains several challenges in implementing the observer (13) though, one of which is how to obtain the output y. Recall that y is defined in (10), and it includes the roll angle ϕ with respect to the horizon, or the Euler roll angle of the vehicle. While the Euler roll angle can be calculated by utilizing a global positioning system (GPS) device [17], [18], such a device is not at all common and/or cost effective in current. Thus, the Euler roll angle that feeds the observer has to be estimated using sensor signals available in production vehicles, which include a steering wheel angle signal, a yaw rate signal, a lateral acceleration signal, and a vehicle speed signal. The estimation algorithm utilizes the kinematic relationship among the signals as well as a bicycle model. It is worth to mention that the roll rate sensor signal, which is being monitored, is not used in the estimation. This is quite necessary since the roll angle estimate is used to cross check the roll rate signal, loosely speaking. Its accuracy should not be affected by the roll rate sensor fault. In Section IV ((29) to be specific), an analysis of the residual will make it clear quantitatively that if df_ϕ/dt were equal to $f_{\dot\phi}$, the residual would not indicate any fault.

A reasonable search within the literature reveals that few studies/documentations discuss the estimation of vehicle roll angle. Among them, Fukada [19] first estimated roll angle by comparing an estimated lateral velocity derivative with the difference between lateral acceleration and the product of yaw rate and vehicle speed. The lateral velocity derivative estimate he used, in turn, depends on a low-pass filter version of the estimated roll angle. Nishio *et al.* [20] used a low-pass filter version of the difference between lateral acceleration and the product of yaw rate and vehicle speed as a roll angle estimate. Tseng [21] first provided a roll angle estimate independent of a side slip angle estimation. In this paper, the calculation of the road bank estimate proposed in [21] is further improved.

Consider a vehicle traveling on a banked road (see Fig. 1). Assuming that the lateral accelerometer is mounted at the vehicle center of gravity (c.g.), its measurement is given by

$$a_y = \dot v + u \cdot \omega_z + g \cdot \sin\phi \tag{15}$$

where a_y is the measured lateral acceleration, u is the longitudinal velocity, ω_z is the yaw rate, v is the lateral velocity, ϕ represents the roll angle, and g is the gravitational constant. Note that in production vehicles, the accelerometer may not be placed at the c.g. due to packaging constraints. Therefore, the output of the sensor may need to be translated to the c.g. location.

From (15), it follows that

$$\sin\phi = (a_y - \dot v - u \cdot \omega_z)/g. \tag{16}$$

However, since $\dot v$ is not available, (16) cannot be implemented but it provides motivations for the subsequent development. A raw roll angle is obtained by assuming $\dot v = 0$, i.e.,

$$\sin\hat\phi_{\text{raw}} = (a_y - u \cdot \omega_z)/g. \tag{17}$$

Obviously, this assumption does not hold true during dynamic vehicle maneuvers, and the calculation (17) may contain significant bias. To overcome this technical difficulty, a dynamic factor DFC, which is more concise than the one used by Tseng [21] is proposed as an indicator of the magnitude of $\dot v$

$$\text{DFC} = \frac{2u^2}{g(L + k_u u^2)} \cdot \left[k_u \cdot a_y + \frac{\omega_z}{u} \cdot L - \delta\right] \tag{18}$$

where L is the wheelbase, δ is the front road wheel angle, and k_u is the understeer coefficient. Note that the expression in the bracket is zero during steady-state cornering if the bicycle model and its nominal understeer coefficient are accurate [22]. While the actual understeer coefficient of a vehicle may deviate from its nominal value, the effect of these variations on DFC can be minimized by choosing the nominal understeer coefficient based on the vehicle's high μ behavior. This is because, in practice, the variation in $k_u \cdot a_y$ is limited since a_y is limited on low μ road surface.

Utilizing DFC, a refined roll angle estimate, $\sin\hat\phi$, can be obtained by modulating the raw estimate $\sin\hat\phi_{\text{raw}}$ as in the following equation [21]:

$$\sin\hat\phi = \sin\hat\phi_{\text{raw}} \cdot \max[0, 1 - |\text{DFC}|]. \tag{19}$$

It can be seen from (19) as the change in lateral velocity increases (indicated by large DFC), the roll angle estimate becomes progressively conservative. This is based on a practical assumption that a vehicle usually does not experience excessive lateral velocity change when experiencing large bank angles, and vice versa. Effectively, this approach eliminates the possible bias introduced by lateral vehicle dynamics.

C. Roll Rate Compensation

It needs to be pointed out that the other variable in (10)—the Euler roll rate $\dot\phi$—is not the same as the roll rate sensor signal. The Euler roll rate is defined in the inertial frame, while the roll rate sensor is attached to the vehicle body and defined in the body frame. Certain maneuvers/road conditions may induce a sensor reading when the vehicle experiences no actual roll motion. In fact, it is quite common that the roll rate sensor would pick up (undesired) roll rate signal from vehicle yaw motion due to a small (e.g., 0.5°) pitch angle caused by sensor misalignment or suspension motion. The opposite is also true, i.e., the vehicle may experience actual roll angle change, but the roll rate sensor measurement is always zero. This can happen when a vehicle makes a U-turn on a very wide, flat but graded driveway. A similar but hypothetical maneuver is described in [17]. Other than the bias introduced by coordinate transformation, the roll rate sensor is subject to an electrical bias. For example, temperature change may cause the output to drift within sensor specification. Therefore, the raw sensor signal, denoted as ω_{x_raw}, should be carefully treated for both the electrical bias and the kinematics-induced bias before it can be applied to the observer in order to avoid false detection.

1) Compensation of the Electrical Bias: The raw roll rate signal ω_{x_raw} needs to be compensated by removing the unknown electrical bias of the sensor

$$\omega_x = \omega_{x\_\mathrm{raw}} - \hat{\varepsilon} \tag{20}$$

where $\hat{\varepsilon}$ represents the estimate of the electrical bias. The following parameter adaptation law is applied to adjust $\hat{\varepsilon}$ so that ω_x is forced to go to zero in the absence of vehicle maneuvering

$$\frac{d\hat{\varepsilon}}{dt} = \gamma_\varepsilon \cdot \omega_x \tag{21}$$

where γ_ε is the parameter adaptation rate. Consider the following positive definite function:

$$V_\varepsilon = \frac{1}{2} \cdot \omega_x^2. \tag{22}$$

From (20) and (21), its time-derivative is easily found to be

$$\frac{dV_\varepsilon}{dt} = -\omega_x \cdot \frac{d\hat{\varepsilon}}{dt} = -\gamma_\varepsilon \cdot \omega_x^2 = -2 \cdot \gamma_\varepsilon \cdot V_\varepsilon. \tag{23}$$

Note that dV_ε/dt in (23) is evaluated under the assumption that ω_{x_raw} is a constant in the absence of maneuvering, which holds true since sensor electrical bias changes much slower than other variables in the system. Under such a condition, one could conclude from (23) that the system defined by (20) and (21) is exponentially stable. Otherwise, if the vehicle is in a maneuver, the structure of the equations guarantees bounded-input bounded-output stability.

2) Compensation of the Kinematic Bias: The roll rate signal generated from the onboard gyro sensor contains a kinematic bias, a quantity relating the inertial frame and the vehicle body frame. Since the roll rate of interest is the one with respect to the inertial frame, a proper compensation has to be performed to remove this kinematics-induced bias, which is mostly the product of pitch angle θ and yaw rate ω_z. To be exact, the Euler roll rate (with respect to the inertial frame) is [23]

$$\dot{\phi} = \omega_x + \omega_y \cdot \sin\phi \cdot \tan\theta + \omega_z \cdot \cos\phi \cdot \tan\theta \tag{24}$$

where ω_y is the pitch rate in the vehicle body frame. Note that ω_x is obtained from (20). To illustrate the significance of this bias removal, consider a vehicle going down a spiraled parking ramp of 6° grade with a yaw rate of, say, 10 °/s. The roll rate sensor will read as much as 1 °/s even though the vehicle stays truly parallel to the parking ramp all the time. In a different scenario, a sensor with a small pitch misalignment of 3° can produce as much as 3 °/s roll rate sensor reading during a constant radius turning maneuver where yaw rate is 60 °/s. Since this bias is kinematics-induced and not a fault of the roll rate sensor, it should be compensated to avoid being interpreted as a fault. Therefore, the following compensation is performed so that the right roll rate signal is fed into the designed observer (13).

If both ω_y and ϕ are small, (24) can be simplified to obtain a kinematically corrected roll rate $\dot{\phi}_{\mathrm{corr}}$

$$\dot{\phi}_{\mathrm{corr}} = \omega_x + \hat{\vartheta} \cdot \omega_z \tag{25}$$

where $\hat{\vartheta}$ represents the estimate of $\tan\theta$. The following parameter adaptation law is applied to adjust $\hat{\vartheta}$ so that $\dot{\phi}_{\mathrm{corr}}$ is forced to go to zero in steady state

$$\frac{d\hat{\vartheta}}{dt} = -\gamma_\vartheta \cdot \dot{\phi}_{\mathrm{corr}} \cdot \omega_z \tag{26}$$

where γ_ϑ is the adaptation rate. Consider the following positive definite function:

$$V_\vartheta = \frac{1}{2} \cdot \dot{\phi}_{\mathrm{corr}}^2. \tag{27}$$

Similar to (23), its time-derivative is given by

$$\begin{aligned} \frac{dV_\vartheta}{dt} &= \dot{\phi}_{\mathrm{corr}} \cdot \frac{d}{dt}(\omega_x + \hat{\vartheta} \cdot \omega_z) \\ &= \dot{\phi}_{\mathrm{corr}} \cdot \frac{d\hat{\vartheta}}{\quad} \cdot \_\_ \\ &= \_\_ \cdot \_\_ \cdot \_\_ \\ &= \_\_ \cdot \_\_ \cdot \_\_ \cdot \_\_ \end{aligned} \tag{28}$$

Therefore, when the vehicle is in a steady-state turn with none zero yaw rate, the system defined by (25) and (26) is exponentially stable. In (28), the fact that ω_x and ω_z are constants in a steady-state turn is used. Note that the vehicle steady-state turning condition is detectable by monitoring other sensor signals such as yaw rate, lateral acceleration, steering wheel angle, etc. During normal driving, there are sufficient steady-state vehicle operating windows for $\hat{\vartheta}$ adaptation.

IV. Simulation Results

In this section, a simulation study, in which the residual generator (13) is applied to system (9) and (10), is conducted in an effort to illustrate the robust fault detection scheme presented in Section III.

Since the residual generator (13) satisfies the disturbance decoupling condition (6), the lumped disturbance term $\tilde{d}$ would not affect the residual. Analyzing of the residual by substituting (14) into (5), further reveals that

$$\begin{aligned} r &= \_\_ \cdot \_\_ \cdot \_\_ \cdot \_\_ \cdot \_\_ \\ &\quad - \frac{\_}{s+\lambda_1} f_\phi - \frac{1}{s+\lambda_1} f_{\dot{\phi}}. \end{aligned} \tag{29}$$

The previous equation shows that the residual is most sensitive to low frequency roll rate sensor fault $f_{\dot{\phi}}$ (*which is the critical failure mode*) and high frequency roll angle estimation error f_ϕ (*which seldom occurs in normal driving*). Such a frequency domain separation of the sensor fault and estimation error is very important from the robustness standpoint. It can be seen that the transfer function from f_ϕ and $f_{\dot{\phi}}$ to residual is determined by

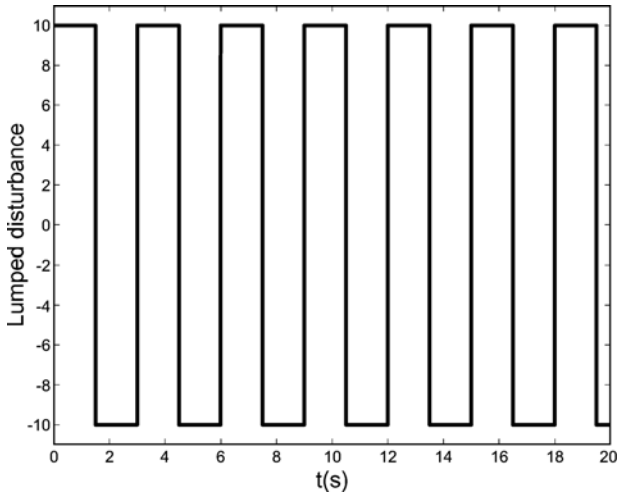

Fig. 2. Simulation: disturbance.

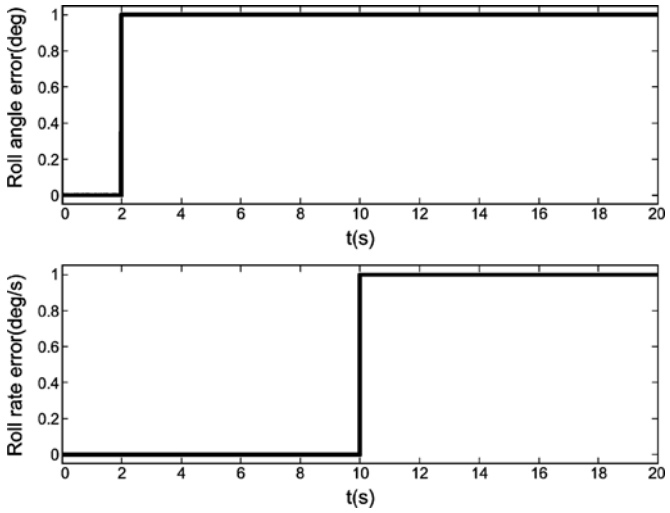

Fig. 3. Simulation: sensor faults.

λ_1 only, and is independent of the parameters in the A matrix of (12). When selecting the observer poles, note that λ_1 should not be too large otherwise the dc gain of $1/s+\lambda_1$ will be reduced. On the flip side, if λ_1 is too small, it will be difficult to separate $f_{\dot{\phi}}$ from f_ϕ due to reduced bandwidth of both $s/s+\lambda_1$ and $1/s+\lambda_1$. A point made earlier and worth repeating here by observing (29), is that caution should be taken when estimating the roll angle so that sf_ϕ does not cancel $f_{\dot{\phi}}$.

The following design parameters and nominal values are used in the simulation:

$$\lambda_1 = 0.7 \quad \lambda_2 = 1 \quad k = 200 \quad c = 100. \tag{30}$$

The system (9) being diagnosed is subject to large parametric uncertainties, i.e., $\Delta k = -300+50\sin(0.5t)$ and $\Delta c = -400+100\cos(0.2t)$. It is also subject to an external square wave disturbance d as shown in Fig. 2. In addition to that, the roll rate sensor "fails" during the simulation, and the roll angle estimate has an error. As shown in Fig. 3, roll angle estimation error f_ϕ is a 1° shift that occurs at $t = 2$ s and roll rate sensor fault $f_{\dot{\phi}}$ is a 1 °/s shift that occurs at $t = 10$ s. The absolute value of the residual is shown in Fig. 4, noting how the residual is insensitive to model uncertainties (i.e., Δk, Δc, and d) due to the disturbance decoupling condition (6), and how it reacts differently to f_ϕ at $t = 2$ s and to $f_{\dot{\phi}}$ at $t = 10$ s, i.e., f_ϕ corresponds to a transient response only while $f_{\dot{\phi}}$ causes a steady-state shift of the residual, which agrees with the analysis (29).

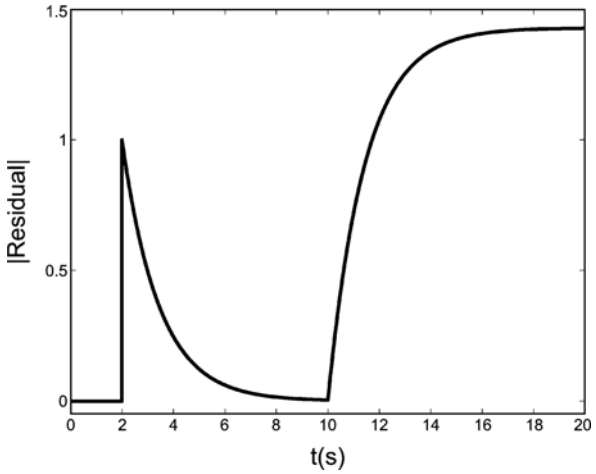

Fig. 4. Simulation: residual.

V. Experimental Verifications

In the literature, successfully implemented or in-production automotive motion sensor fault detection has often been done through voting schemes or information-based fault detection schemes. A similar detection strategy was considered in the early stage of RSC development but soon dropped due to robustness concerns. The reason is given as follows. Suppose a single mass-spring-damper suspension (or sprung mass) model [16] is used to model the vehicle roll dynamics, and the relationship between the suspension roll rate and roll angle can be established. Since only the vehicle roll angle generated from lateral tire force is of interest as far as RSC is concerned, lateral acceleration a_y is the sole input to this model (i.e., bump or vertical force induced vehicle roll is not described)

$$\frac{d}{} \qquad\qquad y \tag{31}$$

where $\dot{\hat{\phi}}_s$ and $\hat{\phi}_s$ represent the suspension roll rate and roll angle estimate, respectively; k_s and c_s are spring stiffness and damping coefficient, respectively; I_x is the sprung mass roll moment of inertia; M is the mass of the sprung mass; h is the distance between the sprung mass center and roll center. The idea is to compare roll rate sensor output to $\dot{\hat{\phi}}_s$ which is independently obtained from the lateral acceleration and the previous model. If the difference between them exceeds a certain threshold, a roll rate sensor fault is suspected. However, external disturbances acting on the vehicle, especially the dynamically changing road super-elevations, prevent the use of such a simple strategy. A real world example is provided to drive the point home. The steering wheel input and the speed of a vehicle maneuvering on

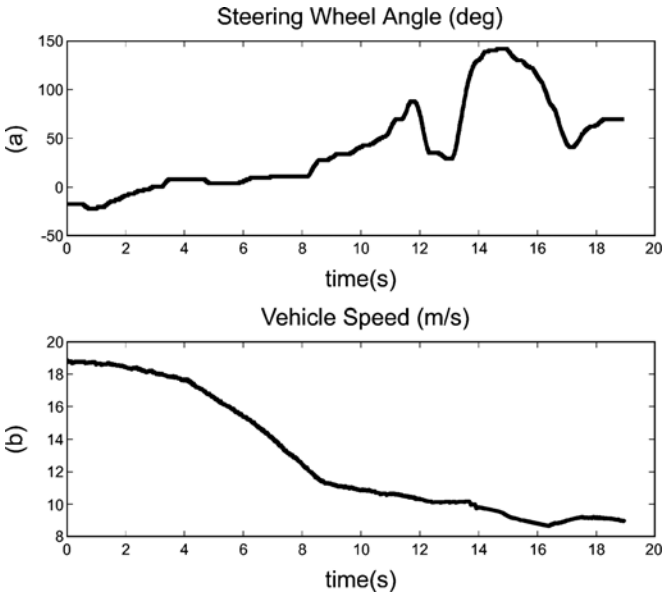

Fig. 5. Experiment: double lane change on a banked road.

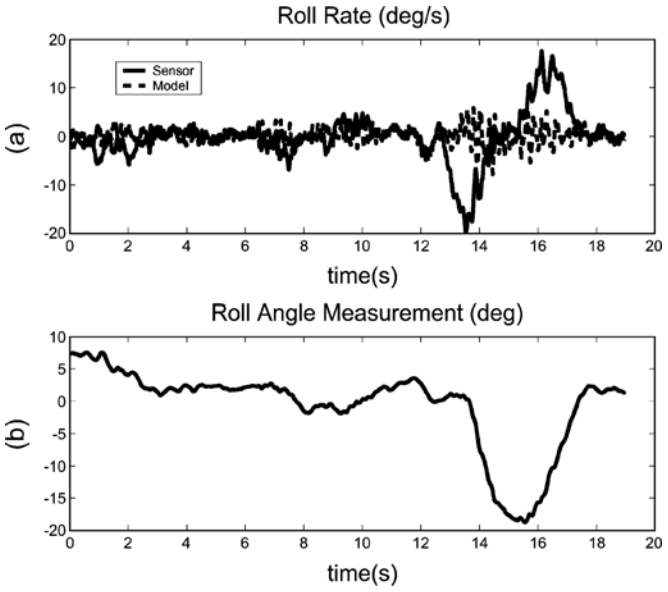

Fig. 6. Experiment: double lane change on a banked road.

a banked road are given by Fig. 5. Due to the road bank disturbance Fig. 6(b), the roll rate from the sensor and roll rate from the model depart from each other Fig. 6(a). A diagnostic decision simply based on such an observation may easily result in a false alarm.

While simulation results in Section IV confirm the robust characteristics of the proposed robust observer, vehicle experimental verifications further substantiate real-world robustness and quantify the impact of road/vehicle/maneuvers disturbances. The proposed residual generator (13) is implemented with $y = [\hat{\phi}\ \dot{\phi}_{\text{corr}}]^T$, where $\hat{\phi}$ is the roll angle estimate from (19) and ϕ_{corr} is the corrected roll rate sensor signal from (25). Design parameters and nominal values are given in (30). The residual is then compared to a threshold. If the threshold

TABLE I
EXPERIMENTAL RESULTS

Maneuvers	Sensor Fault	Detection	False Alarm
Mountain Drive	$10°/s$	Yes	N/A
Double Lane Change	$10°/s$	Yes	N/A
Constant Radius Turn	$10°/s$	Yes	N/A
Lane Change on Gravel	$10°/s$	Yes	N/A
ABS Braking	$10°/s$	Yes	N/A
Spinning on Packed Snow	N/A	N/A	No
Fishhook	N/A	N/A	No
U-Turn on 40% Grade	N/A	N/A	No
Mountain Drive	N/A	N/A	No
Bounce Sine Sweep	N/A	N/A	No

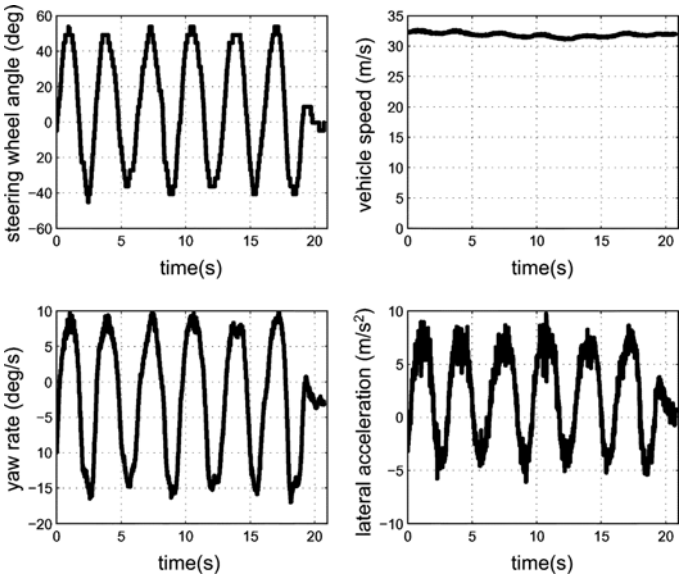

Fig. 7. Experiment: vehicle states (slalom on banked surface).

is exceeded by the residual, the sensor is suspected to be at fault. In general, the threshold should be constructed based on the vehicle dynamics as well as the sensor specification. The basic requirement for the threshold is that it allows for possible vehicle parameter variations and sensor offset/drift within the specification. Furthermore, a dynamic threshold depending on the vehicle states may have a performance/robustness advantage. The idea is to keep the threshold tight for fast fault detection, when the vehicle is operating under normal conditions such as during regular driving on normal road surfaces. When the vehicle is maneuvering on highly banked surfaces or is unstable, the threshold can be increased since these situations are much less frequent than normal driving.

The experimental verifications of no false positive and/or no false negative were performed for a variety of maneuvers and road conditions using several vehicle test platforms. A few representative test results, especially the most challenging ones, are listed in Table I as examples. Fig. 7 shows an aggressive slalom maneuver of a small SUV on a parabolically banked road (whose bank angle varies from 0 to 25° depending on the vehicle's lane positions). This test is especially challenging to

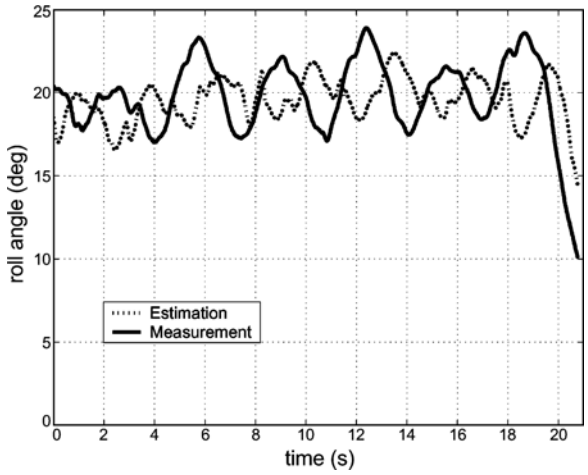

Fig. 8. Experiment: estimated road bank angle.

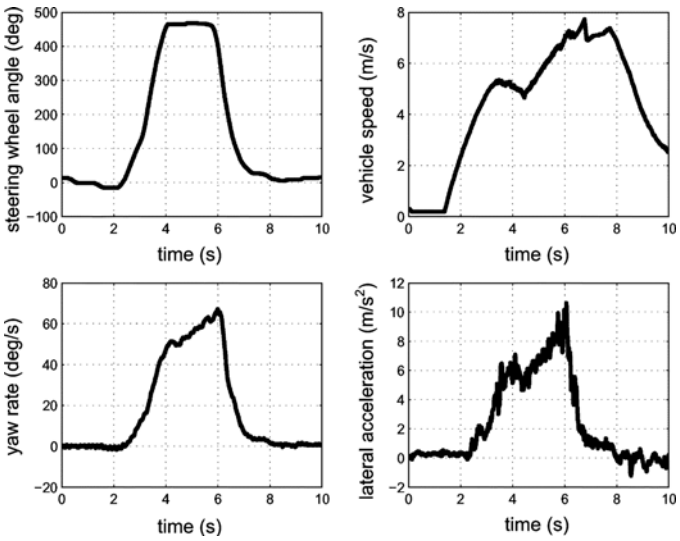

Fig. 9. Experiment: vehicle states (U-turn on 40% grade).

the robustness of the algorithm due to the difficulties in estimating correct vehicle roll angle during the maneuver which involves large and dynamically varying road bank angle (shown in Fig. 8). The test results have verified that there is no false alarm, thanks to the proposed novel roll angle estimation technique and robust fault observer design. Fig. 9 shows a U-turn maneuver on a 40% grade, during which the vehicle traveled down the grade first and then made a sharp U-turn to go up the grade. Due to large pitch angle and high yaw rate, the roll rate sensor signal includes a significant kinematics-induced bias—see (24) or (25). Fig. 10 indicates that no false alarm was present during this test. The results of a fishhook maneuver are given in Figs. 11 and 12 which further verify the robustness of the proposed design.

The experimental verifications of fault detection listed in Table I are illustrated by Figs. 13–16. Fig. 13 shows a high lateral acceleration (a_y =0.7 g between 2 s and 5 s) quasi-steady-state cornering maneuver on dry asphalt. A 10 °/s roll rate fault was inserted during the maneuver and was promptly detected by the increased (and sustained) residual shown in Fig. 14. Fig. 15 shows a dynamic double lane change

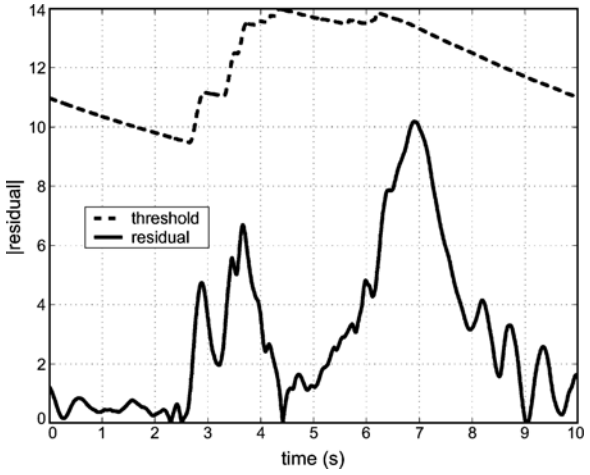

Fig. 10. Experiment: residual and threshold (U-turn on 40% grade).

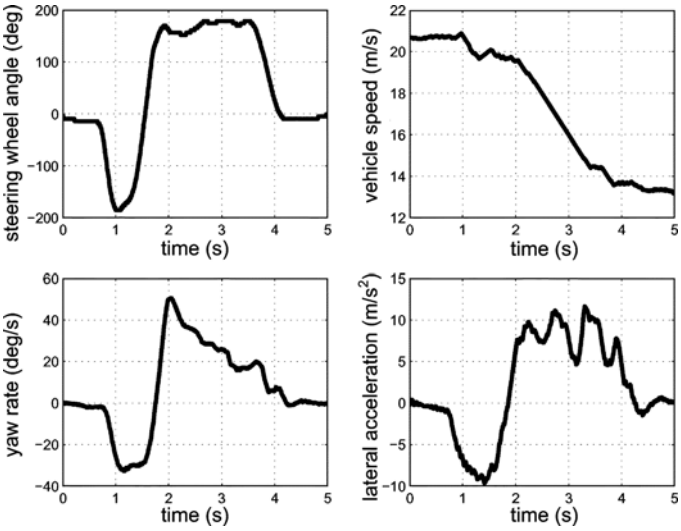

Fig. 11. Experiment: vehicle states (fishhook).

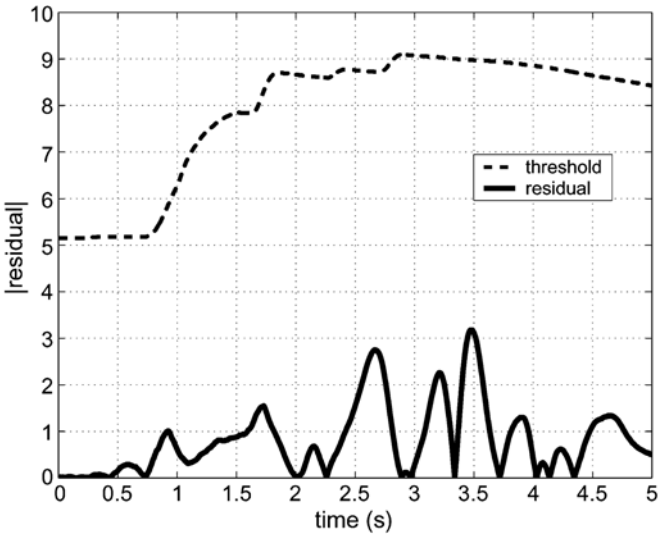

Fig. 12. Experiment: residual and threshold (fishhook).

maneuver of a large SUV on a gravel surface. Despite the very dynamic nature of this maneuver and low road surface μ, the

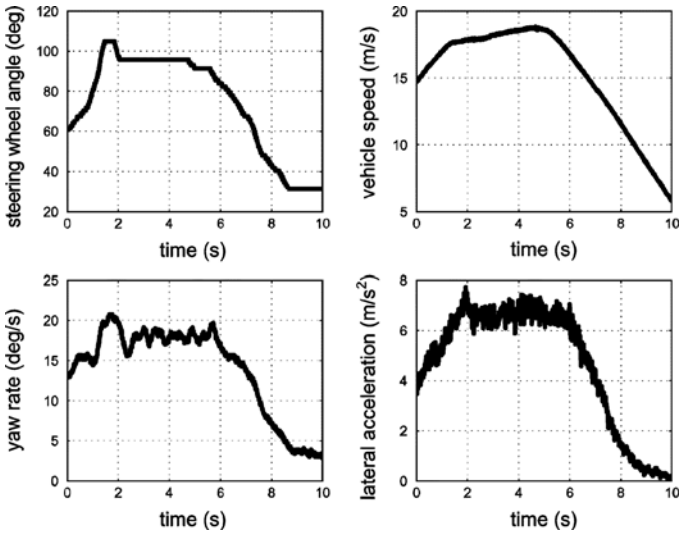

Fig. 13. Experiment: vehicle states (0.7 g constant radius turn).

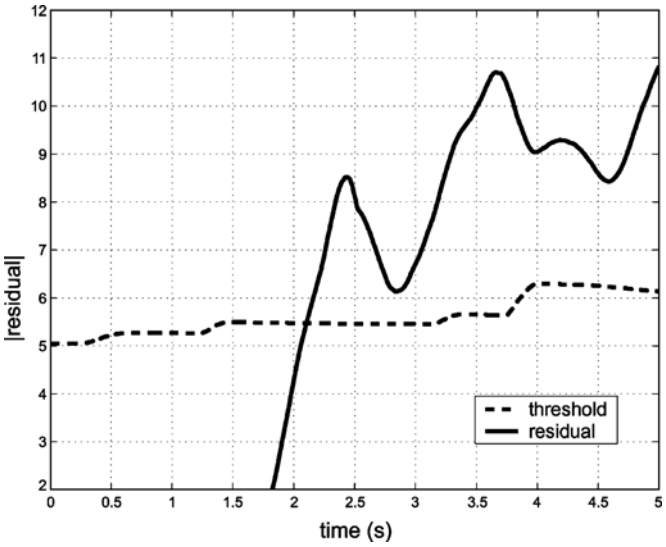

Fig. 16. Experiment: residual and threshold (double lane change).

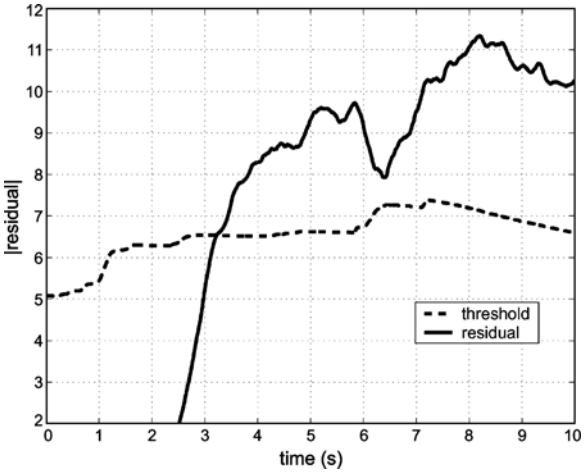

Fig. 14. Experiment: residual and threshold (0.7 g constant radius turn).

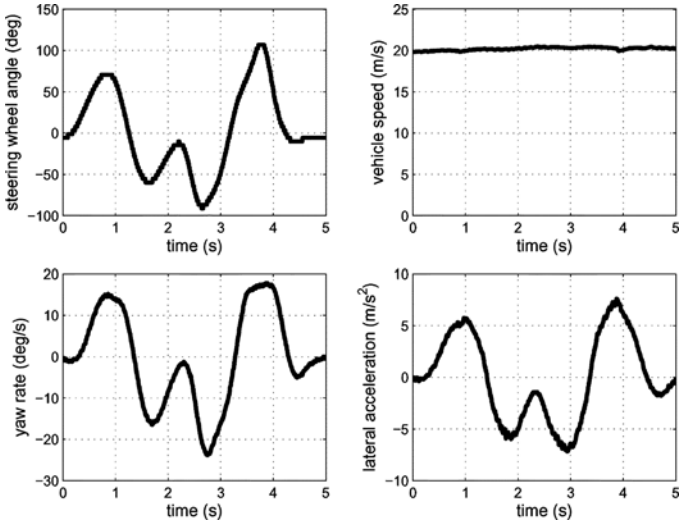

Fig. 15. Experiment: vehicle states (double lane change).

residual exceeded the threshold following the insertion of a 10°/s roll rate fault (Fig. 16).

VI. Conclusion

A model-based fault detection scheme has been presented to detect roll rate sensor failures in a vehicle roll stability control system. The method is based on a simple control-oriented vehicle roll model which is suitable for real-time diagnostic applications. A robust residual generator using eigenstructure assignment is constructed to make the detection insensitive to model uncertainties. The challenges of implementing this strategy are discussed and addressed. Vehicle test results are presented to illustrate the effectiveness and the achievable performance of the proposed scheme.

Acknowledgment

The authors would like to thank the members of the Roll Stability Control (RSC) Development Team at Ford and Volvo, who assisted them in performing extensive vehicle testing and provided invaluable feedbacks. The authors would also like to thank the anonymous reviewers for their constructive comments that lead to the improvement of this paper.

References

[1] T. Brown and D. Rhode, "Roll over stability control for an automotive vehicle," U.S. Patent 6 324 446, Nov. 27, 2001.
[2] H. E. Tseng, B. Ashrafi, D. Madau, T. Brown, and D. Recker, "The development of vehicle stability control at Ford," *IEEE/ASME Trans. Mechatronics*, vol. 4, no. 3, pp. 307–328, Sep. 1999.
[3] R. Isermann, "Process fault detection based on modeling and estimation methods: A survey," *Automatica*, vol. 20, no. 4, pp. 387–404, 1984.
[4] G. G. Leininger, "Model degradation effects on sensor failure detection," in *Proc. Joint Autom. Control Conf.*, 1981, paper FP-3A.
[5] R. J. Patton and J. Chen, "Robust fault detection of jet engine sensor systems using eigenstructure assignment," *J. Guid., Control, Dyn.*, vol. 15, no. 6, pp. 1491–1497, 1992.
[6] R. Patton, P. Frank, and R. Clark, *Fault Diagnosis in Dynamic Systems: Theory and Applications*. London, U.K.: Prentice-Hall Int., 1989.

[7] A. Hac, T. Brown, and J. Martens, "Detection of vehicle rollover," SAE, Int., Warrendale, PA, 2004-01-1757, 2004.
[8] P. Schubert, D. Nichols, E. Wallner, H. Kong, and J. Schiffmann, "Electronics and algorithms for rollover sensing," SAE, Int., Warrendale, PA, 2004-01-0343, 2004.
[9] A. S. Willsky, "A survey of design methods for failure detection in dynamic systems," *Automatica*, vol. 12, no. 6, pp. 601–611, 1976.
[10] J. Gertler, "Survey of model-based failure detection and isolation in complex plants," *IEEE Control Syst. Mag.*, vol. 8, no. 6, pp. 3–11, Dec. 1988.
[11] P. M. Frank and X. Ding, "Survey of robust residual generation and evaluation methods in observer-based fault detection systems," *J. Process Control*, vol. 7, no. 6, pp. 403–424, 1997.
[12] R. C. Montgomery and A. K. Caglayan, "A self-reorganizing digital flight control system for aircraft," presented at the AIAA 12th Aerosp. Sci. Meeting, Washington, DC, 1974.
[13] R. K. Mehra and I. Peshon, "An innovations approach to fault detection and diagnosis in dynamic systems," *Automatica*, vol. 7, pp. 637–640, 1971.
[14] R. J. Patton and J. Chen, "On eigenstructure assignment for robust fault diagnosis," *Int. J. Robust Nonlinear Control*, no. 10, pp. 1193–1208, 2000.
[15] R. Eger, R. Majjad, and N. Nasr, "Rollover simulation based on a nonlinear model," SAE, Int., Warrendale, PA, 980208, 1998.
[16] J. Bernard, J. Shannan, and M. Vanderploeg, "Vehicle rollover on smooth surfaces," SAE, Int., Warrendale, PA, 891991, 1989.
[17] J. Ryu and J. C. Gerdes, "Estimation of vehicle roll and road bank angle," in *Proc. Amer. Control Conf.*, 2004, pp. 2110–2115.
[18] J. O. Hahn, R. Rajamani, S. H. You, and K. I. Lee, "Road bank angle estimation using disturbance observer," in *Proc. 6th Int. Symp. Adv. Veh. Control (AVEC)*, 2002, pp. 381–386.
[19] Y. Fukada, "Estimation of vehicle side-slip with combination method of model observer and direct integration," in *Proc. 4th Int. Symp. Adv. Veh. Control (AVEC)*, 1998, pp. 201–206.
[20] A. Nishio, K. Tozu, H. Yamaguchi, K. Asano, and Y. Amano, "Development of vehicle stability control system based on vehicle sideslip angle estimation," SAE, Int., Warrendale, PA, 2001-01-0137, 2001.
[21] H. E. Tseng, "Dynamic estimation of road bank angle," in *Proc. 5th Int. Symp. Adv. Veh. Control (AVEC)*, 2000, pp. 421–428.
[22] J. Y. Wong, *Theory of Ground Vehicles*, 3rd ed. New York: Wiley, 2001.
[23] D. T. Greenwood, *Principles of Dynamics*, 2nd ed. Englewood Cliffs, NJ: Prentice-Hall, 1988.

Li Xu received the B.S. degree from the University of Electronic Science and Technology of China, Chengdu, China, the M.S. degree from Tsinghua University, Beijing, China, and the Ph.D. degree from Purdue University, West Lafayette, IN, in 1991, 1997, and 2001, respectively, all in mechanical engineering.

Currently, he is with Ford Research and Advanced Engineering, Dearborn, MI, where he is a Research Engineer and has been engaged in several projects on vehicle active safety, chassis modeling and controls.

Hongtei Eric Tseng received the B.S. degree from National Taiwan University, Taipei, Taiwan, in 1986 and the M.S. and Ph.D. degrees from the University of California, Berkeley, in 1991 and 1994, respectively, all in mechanical engineering.

In 1994, he joined Ford Motor Company, Dearborn, MI, where he is currently a Technical Leader at the Research and Innovation Center. His previous work includes low pressure tire warning system using wheel speed sensors, traction control, electronic stability control, and roll stability control. His current research interests include both powertrain and vehicle dynamics control.